Hydrogen dynamics and light-induced structural changes in hydrogenated amorphous silicon

T. A. Abtew* and D. A. Drabold†
Department of Physics and Astronomy, Ohio University, Athens, Ohio 45701, USA
(Received 6 December 2005; revised manuscript received 10 May 2006; published 1 August 2006)

We use accurate first-principles methods to study the network dynamics of hydrogenated amorphous silicon, including the motion of hydrogen. In addition to studies of atomic dynamics in the electronic ground state, we also adopt a simple procedure to track the H dynamics in light-excited states. Consistent with recent experiments and computer simulations, we find that dihydride structures are formed for dynamics in the light-excited states, and we give explicit examples of pathways to these states. Our simulations appear to be consistent with aspects of the Staebler-Wronski effect, such as the light-induced creation of well-separated dangling bonds.

DOI: 10.1103/PhysRevB.74.085201 PACS number(s): 61.43.−j, 66.30.−h, 71.23.−k, 78.20.Bh

I. INTRODUCTION

A variety of experiments and modeling studies of light-induced structural changes in hydrogenated amorphous silicon (*a*-Si:H) reveal the complexity of photoresponse in these materials. Light-induced changes in photoconductivity and defect formation,[1–3] enhanced hydrogen diffusion,[4–9] and creation of preferential proton separation[10] are among the phenomena observed experimentally in *a*-Si:H. A special feature of these materials is the Jekyll-Hyde behavior of hydrogen as a defect passivator enabling the practical utilization of the material but also as a culprit in light-induced defect creation.[11–14] A variety of experiments implicate H and its dynamics[15] as being an important player to the Staebler-Wronski effect.[16]

There are various models proposed to explain the light-induced metastability. Chang *et al.*[17–19] suggested that the dissociation of a two-hydrogen interstitial complex, (H_2^*), into separate and more mobile H atoms, caused by carriers localized on the H_2^*, is a mechanism for the metastable phenomena. In the hydrogen flip model, Biswas *et al.* demonstrated a higher-energy metastable state is formed when H is flipped to the backside of the Si-H bond at a monohydride site.[20] In the hydrogen collision model proposed by Branz,[6] the recombination-induced emission of H from the Si-H bond creates mobile H and dangling bonds, and these newly created dangling bonds become metastable when two mobile H atoms collide to form a complex containing two Si-H bonds. The two-phase model of Zafar and Schiff[21,22] explained thermal stability data, exploited the concept of paired hydrogen, and later merged with the Branz model and invoked dihydride bonding.[23] Though they have different detailed mechanisms for the formation of the structures, the Zafar-Schiff and Branz pictures share the same notion that the diffusion of H and H pair formation plays a key role in light-induced metastability. From *ab initio* simulation in a photoexcited state, Fedders, Fu, and Drabold showed that changes of the charge state of well-localized defect states could induce defect creation.[24] Our work can be regarded as a natural extension of Ref. 24 to the case of a hydrogenated system, and with more accurate techniques than those available at the time of the original study.

Our work has been particularly motivated by the experimental research of Su *et al.*,[10] who performed proton NMR experiments in *a*-Si:H and found preferential light-induced creation of the H-H distance of 2.3±0.2 Å. We have shown that SiH_2 configurations in the solid state are consistent with these observations.[25] More recently, an NMR study by Bobela *et al.*[26] indicated a shorter proton-proton distance in a sample of *a*-Si:H with a somewhat higher defect density.

In a recent paper,[27] we briefly reported the hydrogen dynamics and light-induced formation of a SiH_2 structure for a small (71-atom) model. In this paper, we provide a detailed simulation of electronic properties, vibrational properties, and the mechanism of hydrogen diffusion in both the electronic ground state and light excited state in *a*-Si:H using two different supercell models: a 223-atom *a*-Si:H model (henceforth named Model I) and a 71-atom *a*-Si:H model (Model II). We start with small but topologically credible models of *a*-Si:H and use a sufficiently accurate method to simulate network dynamics, including the diffusive motion of hydrogen. In a photoexcited MD simulation, we find enhanced H motion and formation of paired-H final states, a confirmation of aspects of some current influential models.[6] Furthermore, we obtain final states with additional dangling-bond defects, well separated from each other, again in agreement with key experiments.[28] Our simulations suffer from limitations: small cells and certainly a limited sampling of the possible motions of H, limited simulation times, and approximations of various forms described below. Nevertheless, we believe that studies of this type offer significant promise as an "unbiased" means to discover the importance of H motion, its topological and electronic consequences.

The rest of the paper is organized as follows. In Sec. II, we discuss the approximations used in the *ab initio* local basis code SIESTA,[29–31] describe the procedure for generating the models, and discuss the methods used to simulate both the electronic ground state and the light excited state. In Sec. III, we present a detailed discussion of the molecular-dynamics calculations of hydrogen dynamics and its consequences both in the electronic ground state and in the presence of light excitation. The change in the electronic structures and vibrational modes are explained in detail. We present conclusions in Sec. IV.

II. METHODOLOGY

A. Total energies, electronic structure, and dynamical simulation

Simulation of *a*-Si:H *requires* accurate interatomic interactions (H energetics is highly delicate in *a*-Si:H).[32,33]

 ©2006 The American Physical Society

Therefore, our density-functional simulations were performed within the generalized gradient approximation[34] (GGA) or the local-density approximation (LDA) using the first-principles code SIESTA.[29–31] Norm-conserving Troullier-Martins[35] pseudopotentials factorized in the Kleinman-Bylander[36] form were used. All calculations in this paper employed optimized double-ζ polarized basis sets (DZP), where two s and three p orbitals for the H valence electron and two s, six p, and five d orbitals for Si valence electrons were used. The structures were relaxed until the forces were less than 0.04 eV/Å. We used a plane-wave cutoff of 100 Ry for the grid (used for computing multicenter matrix elements) with 10^{-4} for the tolerance of the density matrix in self-consistency steps. We solved the self-consistent Kohn-Sham equations by direct diagonalization of the Hamiltonian and a conventional mixing scheme. The Γ point was used to sample the Brillouin zone in all calculations.

Density-functional theory in the LDA, or with gradient corrections, maps the ground-state many-electron problem onto a system of noninteracting fermions.[37] In principle, the eigenvalues of the resulting single-particle equations are not true excitation energies and the spectral gap between occupied and unoccupied states is well known to be incorrect.[38] Nevertheless, the eigenvectors of the problem (the Kohn-Sham orbitals) have been shown to be very similar to quasiparticle states from GW calculations, in which the self-energy is expressed as a product of the single particle Green's function "G" and the dynamically screened Coulomb interaction "W" as used in many-body calculations.[39] For Si, C, and LiCl, Hybertsen and Louie[40] found 99.9% overlap between GW states and the Kohn-Sham orbitals. On an empirical level for amorphous materials, there are many indications that it is profitable to interpret the Kohn-Sham orbitals "literally" for comparisons to experiment.[41,42] This provides some rationale for interpreting the Kohn-Sham orbitals as quasiparticle states, as we shall in some subsequent parts of this paper.

B. Models

A predictive simulation requires a physically plausible model that represents the topology of the network and yields an accurate description for dynamics of the atoms. In this paper, we have used two different supercell models: a 223-atom a-Si:H model (Model I) and a 71 atom a-Si:H model (Model II). These models are generated from 64-atom and 216-atom a-Si models that were generated by Barkema and Mousseau[43] using an improved version of the Wooten, Winer, and Weaire (WWW) algorithm,[44] respectively.

To create the a-Si:H environment, we did the following. (a) We started from a 216-atom a-Si model with two dangling bonds, and we removed two silicon atoms resulting in the formation of additional vacancies. All of the vacancies except one are then terminated by placing a H atom at about 1.5 Å from the corresponding Si atom. This yielded a 223-atom "Model I." (b) We started from a defect-free 64-atom a-Si model, and we removed three silicon atoms resulting in the formation of vacancies. All of the dangling bonds are then terminated by placing a H atom at about 1.5 Å from the corresponding Si atom to generate a 71-atom "Model II." We then repeated this supercell surgery at other sites to generate an ensemble of three configurations. Finally, these newly generated structures are well relaxed using conjugate gradient optimization. While such a procedure is clearly unphysical, it is worth pointing out that the resulting proton NMR second moments of the proton clusters created are similar to the broad component of the line shape observed in experiments.[45]

C. Ground-state dynamics and promotion of carriers

Defects in an amorphous network may lead to localized electron states in the optical gap or in the band tails. If such a system is exposed to band-gap light, it becomes possible for the light to induce transitions from the occupied states to unoccupied states. For the present work, we will not concern ourselves with the subtleties of how the EM field introduces the transition; we will simply assume that a photoinduced promotion occurs, by depleting the occupied states of one electron "forming a hole" and placing the electron near the bottom of the unoccupied "conduction" states. The idea is that a system initially at equilibrium will not be after the procedure: Hellmann-Feynman forces[46] due to the occupation change will cause structural rearrangements, which may be negligible or dramatic, depending on the flexibility or stability of the network, and the localization of the states. The changes in force will initially be local to the region in which the orbitals are localized, followed by transport of the thermal energy. In general, it is necessary to investigate photostructural changes arising from various different initial and final states, though only well localized states near the gap have the potential to induce structural change.[24,47–50] The simulated light-excited state is achieved in the following steps: (a) starting from the well relaxed model, we make the occupation change by adding an additional electron just above the Fermi level, (b) we keep the system in this excited state for 10 ps (20 000 MD steps with time step τ=0.5 fs between each MD step), and maintain a constant temperature T=300 K, and (c) after 10 ps, we put the system back into the ground state and relax to minimize the energy. The method has been described in additional detail elsewhere.[47] All results reported in this paper are for 10 ps of time evolution.

III. HYDROGEN DYNAMICS

We have performed extensive MD simulations of network dynamics of a-Si:H both in an electronic ground state (what we will call "light-off") and simulated light-excited states ("light-on") for Model I and Model II described above. In the next sections, we present a detailed calculation of hydrogen diffusion, its mechanisms, and consequences on the structural, electronic, and vibrational properties in both the electronic ground state and the light-excited state.

A. Hydrogen motion: Ground state

To analyze the diffusion mechanism in the ground state, we performed a MD simulation for five different tempera-

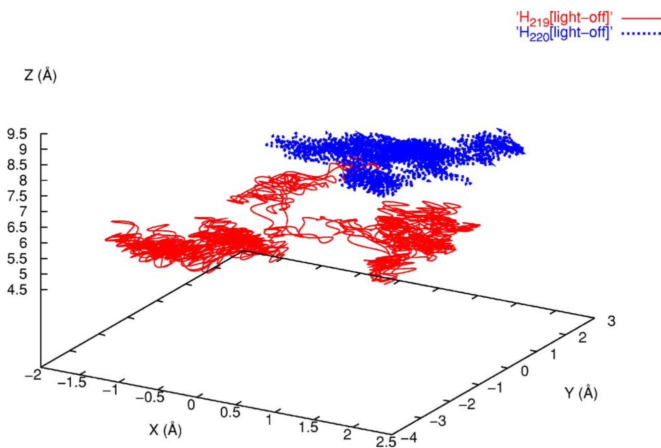

FIG. 1. (Color online) Trajectory for two different hydrogen atoms (H_{219} and H_{220}) in the ground state, which shows the diffusion and trapping of the atom for 223-atom Model I. The total time for the trajectory is 10 ps.

tures, and tracked the trajectories and bonding information of all the H and Si atoms in the network. In all the cases, the MD simulations show diffusion of hydrogen in the cell, and as a consequence, the network exhibits dynamical bond breaking and formation processes. The pattern of diffusion differs for individual H atoms depending upon the geometrical constraints around the diffusing H atom. As expected from crystalline Si, Si-Si bond centers are preferred traps for diffusing H atoms.

In order to graphically characterize the trajectories of H diffusion in the ground state, we have selected two diffusive H atoms (H_{219} and H_{220}), and plotted their trajectories at $T=300$ K in Fig. 1. The trajectories for both H_{219} and H_{220} atoms show diffusion in which the H atoms spend time being trapped in a small volume of the cell, which is followed by rapid emission to another trapping site. In order to examine how the bond rearrangement takes place in the network while the H atom is diffusing, we tracked each hydrogen atom and computed its bonding statistics.

In Fig. 2, we show the Si-H bond length between one of the diffusing H atoms (namely H_{219}) and relevant Si atoms (Si_{90} and Si_{128}) with which it forms a bond while diffusing and Si_{208}. As we can see from Fig. 2, in the first 4 ps H_{219} is bonded with Si_{90} with a bond length of 1.5 Å and trapped for a while until it breaks and hops to form another bond with Si_{128}. In the first ~4 ps, the bond length between H_{219} and Si_{128} fluctuates between 3.8 and 2.5 Å. However, after ~4 ps we observed a swift bond change of ~0.1 ps when the H_{219} atom pops out of the trapping site and hops to form a bond with Si_{128} and is trapped there for ~6 ps. This process of trapping and hopping is typical for the highly diffusive H atoms. These examples reveal the importance of the H hopping, and also show that this simulation by itself is incomplete to provide much information about the statistics of trap lifetimes, absorption, and emission probabilities.

To study atomic diffusion, we computed the time average mean-squared displacement for both H and Si atoms for a given temperature using

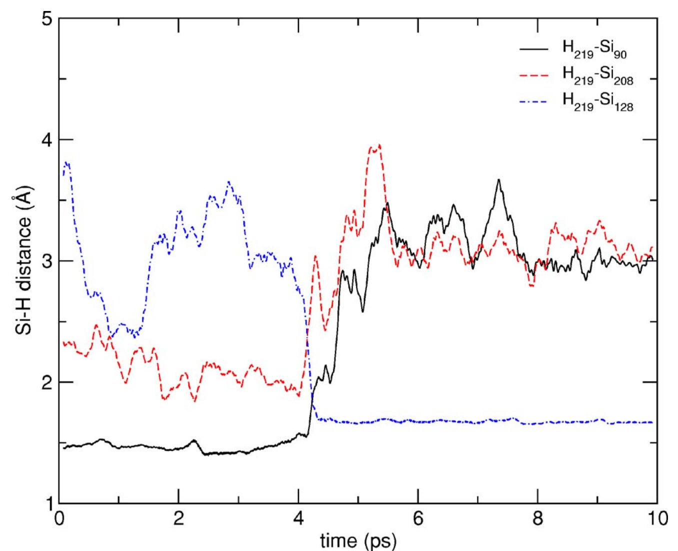

FIG. 2. (Color online) The Si-H bond length between the diffusing H (H_{219}) and three different Si atoms (Si_{90}, Si_{208}, and Si_{128}) as a function of time in the electronic ground state for Model I. The total time for the trajectory is 10 ps.

$$\langle \sigma^2(\alpha,T)\rangle_{\text{time}} = \frac{1}{N_{\text{MD}}}\frac{1}{N_\alpha}\sum_{t=1}^{N_{\text{MD}}}\sum_{i=1}^{N_\alpha}|\vec{r}_i^{\,\alpha}(t) - \vec{r}_i^{\,\alpha}(0)|^2, \tag{1}$$

where the sum is over particular atomic species α (Si or H), N_α and $\vec{r}_i^{\,\alpha}(t)$ are total number and coordinates of the atomic species α at time t, respectively, and N_{MD} is the total number of MD steps.

The time average mean-square displacement for Model II for five different temperatures was calculated using Eq. (1) for H atoms in the supercell in the electronic ground state (light-off) and it is shown in Fig. 3. We have observed a temperature dependence of H diffusion. This result will help us to compare the diffusion of H in the electronic ground

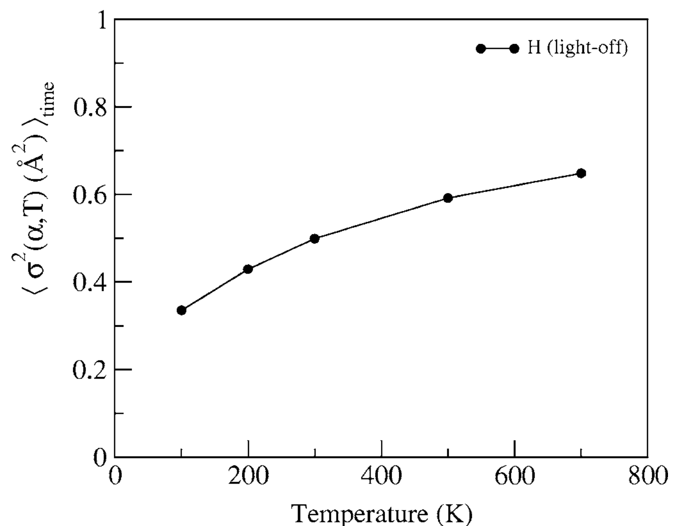

FIG. 3. Time-averaged mean-square displacement for H as a function of temperature of MD simulation in the electronic ground state for 71-atom Model II.

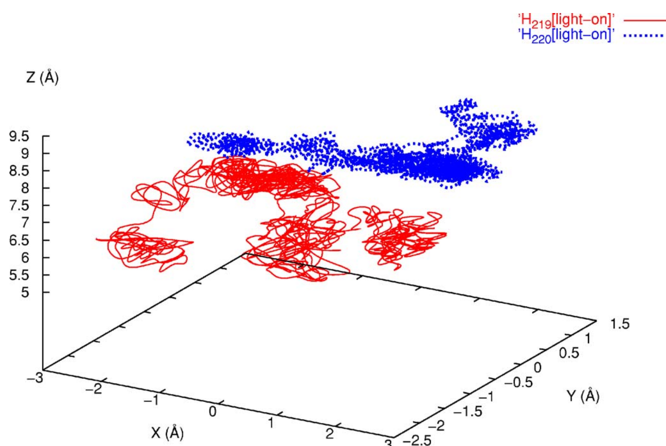

FIG. 4. (Color online) Trajectory for three different hydrogen atoms (H_{219} and H_{220}) which shows the diffusion and trapping of the atom for Model I in the light excited state. The total time for the trajectory is 10 ps.

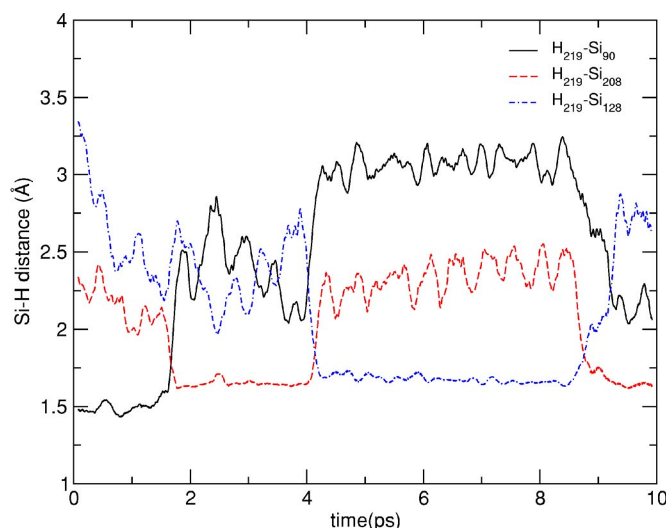

FIG. 5. (Color online) The Si-H bond length between the diffusing H (H_{219}) and three different Si atoms (Si_{90}, Si_{128}, and Si_{208}) with which H_{219} forms a bond (one at a time) while it is diffusing as a function of time for Model I, in the light excited state. The total time for the trajectory is 10 ps.

state with the light-excited state to be discussed in the next section.

B. Hydrogen diffusion: Light-excited state

Similar to the case of the electronic ground state, we analyzed the diffusion of H in the light-excited state. We tracked the trajectories and bonding statistics of Si and H atoms in the supercell. Our MD simulation in the light-excited state shows enhanced hydrogen diffusion and consequently increased bond breaking and formation that leads to structural changes in the network.

We studied the diffusion mechanism of H for the light-excited state case. To illustrate the trajectories of H in the light-excited state, we have again selected two diffusive H atoms (H_{219} and H_{220}) from the larger Model I, and plotted their trajectories in the light-excited state in Fig. 4. The trajectories show the diffusion of H in the presence of different trapping centers, a region where the H atom spends more time before it hops and moves to another trapping site. However, in this case we observed enhanced diffusion and more trapping sites and hopping. These trapping and hopping processes continue until two hydrogens form a bond to a single Si atom to form a metastable SiH_2 conformation or until two hydrogens form a bond to (a) two different Si atoms which are bonded to each other, to form (H-Si-Si-H) structure or (b) two different Si atoms which are not bonded but close to each other. This is a basic event of the H collision model[6] and other H-pairing models.[23]

By tracking each H atom, we computed its bonding statistics and examine the bond rearrangements. In Fig. 5, we show the Si-H bond length as a function of time between one of the diffusing H atoms (H_{219}) and three other Si atoms (Si_{90}, Si_{128}, and Si_{208}) with which it forms a bond while diffusing in the network. The initial trapping time, where H_{219} is bonded with Si_{90}, is reduced to ~1.8 ps when the light is on from ~4 ps when the light is off. This is followed by another trapping event in which H_{219} is bonded with Si_{208} for another ~2.1 ps. The H_{219} hops out of the trapping site and forms a bond with Si_{128} and trapped for ~4.3 ps before it finally hops out from the trapping site and forms another bond with Si_{208} where it gets trapped again and forms a silicon dihydride (SiH_2) structure. From Fig. 5, the pattern of diffusion is quite different from the ground state: In the light-excited state case, we observed (a) more trapping sites and less trapping time with frequent hopping, (b) enhanced hydrogen diffusion, and (c) an increasing number of bond rearrangements and newly formed dihydride structural units.

The atomic diffusion in the light-excited state case has also been examined using the time average mean-squared displacement for both H and Si atoms for different temperatures using Eq. (1) for both Model I and Model II. The result from Model II is shown in Fig. 6. For the temperatures considered, our simulation shows enhanced diffusion of H for the case in which the light is "on" as compared with the case in which the light is "off." Consistent with the work of Isoya,[28] the hopping of H is apparently stimulated in the photoexcited state. The enhanced diffusive motion of H in the photoexcited state relative to the electronic ground state arises from the strong electron-lattice interaction of the amorphous network, and an effect of "local heating" and subsequent thermal diffusion[48] initially in the spatial volume in which the state is localized. The same calculations have also been performed on the larger model, Model I, at $T=300$ K, in which the time average mean-square displacement for H is 2.66 Å^2 for the light-excited state and 1.10 Å^2 for the electronic ground state.

C. Consequences of hydrogen diffusion

1. Formation of dihydride structure

In the two scenarios we considered—MD simulation in the electronic ground state (light off) and the simulated light-excited state (light on)—we have observed an important dif-

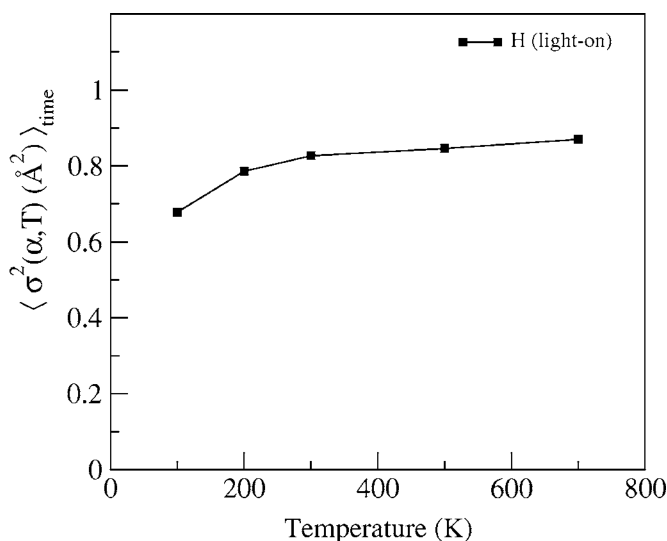

FIG. 6. Time average mean-square displacement for H as a function of temperature of MD simulation in the light excited state for Model II.

ference. In the light-excited state, in addition to bond rearrangements and enhanced hydrogen diffusion, we have observed a preferential formation of new structure: SiH_2, with an average distance of 2.39 Å for the pair of hydrogens in the structure, (H-Si-Si-H) and (H-Si Si-H) with H-H separation which ranges from 1.8 to 4.5 Å. However, in the electronic ground state, we have obtained rearrangement of atoms including hydrogen diffusion, without the formation of SiH_2 structure in the supercell. The formation of these structures in the light-excited state follows breaking of the H atom from the Si-H bond close to the dangling bonds and diffusion to the nearest weakly bonded interstitial sites (or dangling bonds). This mobile H atom then collides (forms a metastable bond) with another Si+DB structure or breaks an Si-Si bond to form another Si-H bond. This is attributed to the fact that the dangling-bond site is moving to accommodate the change in force caused by the additional carrier and also because hydrogen is moving through weakly bonded interstitial sites with low activation barrier for diffusion until it is trapped by a defect.[51]

We find that there are two different modes of bond formation for the mobile hydrogen. The first is when two mobile hydrogen atoms, H_m, collide with two Si atoms and form a metastable (H-Si-Si-H) or (H-Si Si-H) structure, and the second one is when the mobile hydrogen moves until it encounters a preexisting Si-H+DB structure and makes a bond to form a SiH_2 structure. Consequently, our calculations show two basic consequences for the diffusion of H in the light-excited state: (i) the diffusion of hydrogen not only breaks a Si-H bond but also breaks a Si-Si bond and (ii) the possibility that two mobile H atoms might form a bond to a single Si atom to form a metastable SiH_2 structure in addition to the formation of (H-Si-Si-H) and (H-Si Si-H) structures.

In Model II, the two hydrogens involved in the formation of the SiH_2 structure initially were 5.50 Å apart and bonded to two different Si atoms (Si-H), which were separated by 4.86 Å. With thermal simulation in the light-excited state, the two hydrogen atoms dissociate from their original Si atoms and become mobile until they form the SiH_2 structure, in which the H-H distance becomes 2.39 Å. We have observed a similar pattern of H diffusion, bond rearrangements, and formation of SiH_2 structure near the DB for the other two configurations considered in the simulation. The same phenomenon is observed in the case of Model I. The two hydrogens involved in the formation of the SiH_2 structure initially were 3.29 Å apart and bonded to two different Si atoms (Si-H) which were separated by 3.92 Å. With thermal simulation in the light-excited state, the two hydrogen atoms dissociate from their original host and become mobile until they form the SiH_2 structure, in which the H-H distance becomes 2.45 Å. We have summarized the results that show before and after MD calculations of H-H distance (in SiH_2 structure) for Model I and three different configurations of Model II in the case of the light-excited state in Table I.

TABLE I. The H-H distance in the SiH_2 configurations and the Fermi energy of the system before and after MD simulations in the light-excited case.

	H-H distance	
Configurations	Before MD (Å)	After MD (Å)
1 (Model II)	5.50	2.39
2 (Model II)	3.79	2.36
3 (Model II)	4.52	2.36
4 (Model I)	3.29	2.45
Average		2.39

2. Changes in the electronic properties

In order to understand the electron localization, we used the inverse participation ratio, $\mathcal{I}$,

$$\mathcal{I} = \sum_{i=1}^{N} [q_i(E)]^2 \tag{2}$$

where $q_i(E)$ is the Mulliken charge residing at an atomic site i for an eigenstate with eigenvalue E that satisfies $\Sigma_i^N[q_i(E)]=1$ and N is the total number of atoms in the cell. For an ideally localized state, only one atomic site contributes all the charge and so $\mathcal{I}=1$. For a uniformly extended state, the Mulliken charge contribution per site is uniform and equals $1/N$ and so $\mathcal{I}=1/N$. Thus, large $\mathcal{I}$ corresponds to localized states. With this measure, we observe a highly localized state near and below the Fermi level and a less localized state near and above the Fermi level. These states, the highest occupied molecular orbitals (HOMO) and the lowest unoccupied molecular orbitals (LUMO), are centered at the two dangling bonds in the initial configuration of the model. The energy splitting between the HOMO and LUMO states is 1.08 eV. Figure 7(a) shows the Fermi level and $\mathcal{I}$ of these two states and other states as a function of energy eigenvalues in the relaxed electronic ground state.

This picture changes when we excite the system and perform a MD calculation in which we observe enhanced diffu-

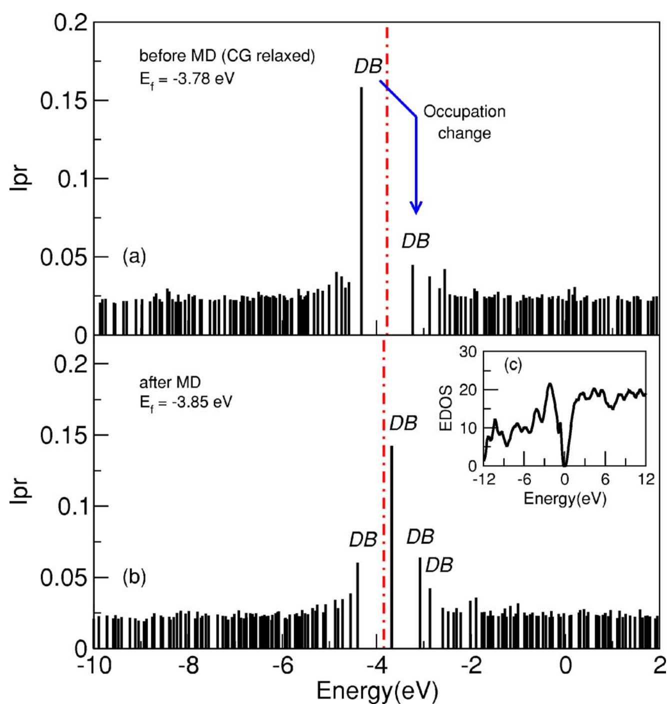

FIG. 7. (Color online) The inverse participation ratio $\mathcal{I}$ of the eigenstates vs the energy eigenvalues, (a) in the relaxed electronic ground state and (b) in the relaxed simulated light-excited state (light-excited MD followed by relaxation), with their respective Fermi energy in the first configuration of relaxed Model II. The inset (c) shows the electron density of states with the Fermi level shifted to zero for the light-excited state with subsequent relaxation.

sion of hydrogen and subsequent breaking and the formation of bonds. Since the electron-lattice coupling is large for localized states,[52] the change of occupation causes the forces in the localization volume associated with the DB to change and the system moves to accommodate the changed force. Consequently, the hydrogen atoms close to the DB sites start to move in the vicinity of these defects either to terminate the old DBs or to break a weak Si-Si bond, and by doing so, create new DB defects on nearby sites. As shown in Fig. 7(b), we observe the formation of a highly localized state and the appearance of three less localized states, which correspond to the newly formed defect levels after simulated light-soaking.

$\mathcal{I}_{\mathrm{HOMO}}$ decreases from 0.158 to 0.060 after photoexcitation, while $\mathcal{I}_{\mathrm{LUMO}}$ increases from 0.045 to 0.142. The splitting energy between the HOMO and LUMO states has also declined to 0.723 eV. The newly formed defects with lower energy splitting between the HOMO and LUMO states suggest a presence of carrier-induced bond rearrangements in the supercell. The comparisons for the energy and $\mathcal{I}$ of the system before MD (as relaxed) and after MD are given in Table II.

In addition, analysis of the spatial distribution of the configurations shows that the H atoms close to the dangling bonds (<4.0 Å) are most diffusive and the Si atoms that make most of the bond rearrangements including the Si atom in the SiH_2 configurations are close (<5.50 Å) to the dangling bonds. These show that the additional charge carrier

TABLE II. The energy and the inverse participation ratio $\mathcal{I}$ of localized states HOMO, LUMO, LUMO+1 and LUMO+2 before and after the MD for Model II.

	Eigenvalue		$\mathcal{I}$	
	Before MD (eV)	After MD (eV)	Before MD	After MD
HOMO	−4.32	−4.40	0.158	0.060
LUMO	−3.24	−3.68	0.045	0.142
LUMO+1	−2.88	−3.08	0.037	0.064
LUMO+2	−2.66	−2.87	0.030	0.042

induces change in the forces around the dangling bonds and consequently rearranges the atoms around the dangling-bond sites and eventually forms an SiH_2 structure. On average, the newly formed defect sites are 3.80 and 4.70 Å far away from the two initial defect sites. The newly formed SiH_2 structure is (on average) 4.11 Å away from the initial defect sites. It is probable that limitations in both length and time scales influence these numbers, but it is clear that the defect creation is *not* very local because of the high diffusivity of the H.

The same calculations have been performed on Model II. In Fig. 8, we have plotted both the energy density of states and the inverse participation ratio as a function of energy in the light-excited state case before and after the MD simulation. As can be seen from the figure, we obtained more localized states in the middle of the gap which are caused due

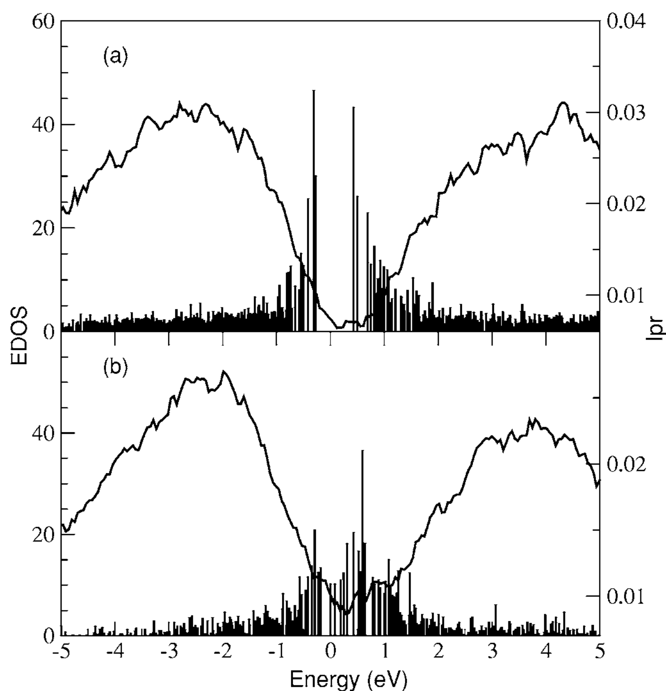

FIG. 8. The energy density of states and inverse participation ratio of the eigenstates vs the energy for Model I, (a) in the relaxed electronic ground state and (b) in the relaxed simulated light-excited state (light-excited MD followed by relaxation); both the electron density of states and the inverse participation ratio are plotted with the Fermi level shifted to zero.

TABLE III. Frequency for some of the Si-H vibrational modes of the SiH_2 conformation for the first two configurations of the Model II obtained from our MD simulations and their corresponding experimental values.[53–55]

Configurations	Rocking (cm^{-1})	Scissors (cm^{-1})	Stretch (cm^{-1})
1	629	810	2025
2	625	706	2047
Experiment	630	875	2090

to an increase in the number of defects upon light excitation. This supports the idea that the diffusion of hydrogen not only forms preferential dihydride structures but also increases the number of defects, in agreement with our findings for the smaller Model II.

3. Change in the vibrational properties

Starting with the relaxed Model II (subsequent to MD in the light-excited state), we computed the vibrational energies and vibrational modes by diagonalizing the dynamical matrix obtained from finite-difference calculations. In our calculations, the VDOS shows H modes in the range 600–900 cm^{-1} and also in the range 1800–2100 cm^{-1}. We have examined the vibrational modes to pick out those modes arising only from SiH_2. We reproduce the vibrational modes of SiH_2 and their corresponding experimental values[53–55] in Table III. The first mode is the rocking mode at 629 and 625 cm^{-1}, the second is the scissors mode at 810 and 706 cm^{-1}, and the last is the asymmetric stretching mode that occurs at 2025 and 2047 cm^{-1} for the first and second configurations, respectively. These results are in good agreement with the IR absorption spectra for the SiH_2 structure. A comparison of our results for the vibrational modes of SiH_2 with the experiment is summarized in Table III. The results shown in Table III are sensitive to the basis sets used in the calculation, in agreement with other work emphasizing the delicacy of H dynamics.[32]

IV. CONCLUSION

We have presented a direct *ab initio* calculation of network dynamics and diffusion both for the electronic ground state and light-excited state for *a*-Si:H. We computed the preferential diffusion pathways of hydrogen in the presence of photoexcited carriers. In the light-excited state, we observe enhanced hydrogen diffusion and the formation of new silicon dihydride configurations, (H-Si-Si-H), (H-Si Si-H), and SiH_2. The two hydrogens in the SiH_2 unit show an average proton separation of 2.39 Å. The results are consistent (a) with the recent NMR experiments and our previous studies, and (b) with the hydrogen collision model of Branz and the other paired hydrogen model in the basic diffusion mechanism and the formation of dihydride structures. In contrast, simulations in the electronic ground state do not exhibit the tendency to SiH_2 formation. This paper discusses two different models (71 and 223 atoms), which differ in quantitative details (such as the sparsely sampled density of band tail states), but agree on key issues such as light-enhanced H diffusion and paired-H formation. Undoubtedly, other H diffusion pathways exist, and the importance of larger simulation length and time scales as well as the effects of promotions involving different states (which could include strain defects and floating bonds[56]) should be undertaken. We show the detailed dynamic pathways that arise from light-induced occupation changes, and provide one explicit example of defect creation and paired H formation.

ACKNOWLEDGMENTS

We acknowledge support from the National Science Foundation under NSF-DMR 0600073, 0605890 and the Army Research Office under MURI W911NF-06-2-0026. We thank E. A. Schiff and H. Branz for helpful conversations and suggestions, and P. A. Fedders and P. C. Taylor for collaboration and discussions.

*Electronic address: abtew@phy.ohiou.edu
†Electronic address: drabold@ohio.edu

[1] D. L. Staebler and C. R. Wronski, Appl. Phys. Lett. **31**, 292 (1977).
[2] M. Stutzmann, W. B. Jackson, and C. C. Tsai, Phys. Rev. B **32**, 23 (1985).
[3] D. Han, J. Baugh, G. Yue, and Q. Wang, Phys. Rev. B **62**, 7169 (2000).
[4] W. B. Jackson and J. Kakalios, Phys. Rev. B **37**, 1020 (1988).
[5] P. V. Santos, N. M. Johnson, and R. A. Street, Phys. Rev. Lett. **67**, 2686 (1991).
[6] H. M. Branz, Phys. Rev. B **59**, 5498 (1999).
[7] H. M. Branz, S. Asher, H. Gleskova, and S. Wagner, Phys. Rev. B **59**, 5513 (1999).
[8] H. M. Cheong, S. Lee, B. P. Nelson, A. Mascarenhas, and S. K. Deb, Appl. Phys. Lett. **77**, 2686 (2000).
[9] M. S. Valipa and D. Maroudas, Appl. Phys. Lett. **87**, 261911 (2005).
[10] T. Su, P. C. Taylor, G. Ganguly, and D. E. Carlson, Phys. Rev. Lett. **89**, 015502 (2002).
[11] K. Zellama, P. Germain, S. Squelard, B. Bourdon, J. Fontenille, and R. Danielou, Phys. Rev. B **23**, 6648 (1981).
[12] M. Kemp and H. M. Branz, Phys. Rev. B **52**, 13946 (1995).
[13] B. Tuttle, C. G. Van de Walle, and J. B. Adams, Phys. Rev. B **59**, 5493 (1999).
[14] Y.-S. Su and S. T. Pantelides, Phys. Rev. Lett. **88**, 165503 (2002).
[15] P. Roura, J. Farjas, C. Rath, J. Serra-Miralles, E. Bertran, and P. Rocai Cabarrocas, Phys. Rev. B **73**, 085203 (2006).
[16] R. A. Street, *Hydrogenated Amorphous Silicon* (Cambridge University Press, Cambridge, UK, 1991).
[17] K. J. Chang and D. J. Chadi, Phys. Rev. Lett. **62**, 937 (1989).
[18] K. J. Chang and D. J. Chadi, Phys. Rev. B **40**, 11644 (1989).

[19] S. B. Zhang, W. B. Jackson, and D. J. Chadi, Phys. Rev. Lett. **65**, 2575 (1990).
[20] R. Biswas and Y.-P. Li, Phys. Rev. Lett. **82**, 2512 (1999).
[21] S. Zafar and E. A. Schiff, Phys. Rev. B **40**, 5235 (1989).
[22] S. Zafar and E. A. Schiff, Phys. Rev. Lett. **66**, 1493 (1991).
[23] N. Kopidakis and E. A. Schiff, J. Non-Cryst. Solids **266-269**, 415 (2000).
[24] P. A. Fedders, Y. Fu, and D. A. Drabold, Phys. Rev. Lett. **68**, 1888 (1992).
[25] T. A. Abtew, D. A. Drabold, and P. C. Taylor, Appl. Phys. Lett. **86**, 241916 (2005).
[26] D. Bobela, T. Su, P. C. Taylor, and G. Ganguly, J. Non-Cryst. Solids **352**, 1041 (2006).
[27] T. A. Abtew and D. A. Drabold, J. Phys.: Condens. Matter **18**, L1 (2006).
[28] J. Isoya, S. Yamasaki, H. Okushi, A. Matsuda, and K. Tanaka, Phys. Rev. B **47**, 7013 (1993).
[29] P. Ordejón, E. Artacho, and J. M. Soler, Phys. Rev. B **53**, R10441 (1996).
[30] D. Sánchez-Portal, P. Ordejón, E. Artacho, and J. M. Soler, Int. J. Quantum Chem. **65**, 453 (1997).
[31] J. M. Soler, E. Artacho, J. D. Gale, A. García, J. Junquera, P. Ordejón, and D. Sánchez-Portal, J. Phys.: Condens. Matter **14**, 2745 (2002).
[32] C. G. Van de Walle, Phys. Rev. B **49**, 4579 (1994).
[33] R. Atta-Fynn, P. Biswas, P. Ordejón, and D. A. Drabold, Phys. Rev. B **69**, 085207 (2004).
[34] J. P. Perdew, K. Burke, and M. Ernzerhof, Phys. Rev. Lett. **77**, 3865 (1996).
[35] N. Troullier and J. L. Martins, Phys. Rev. B **43**, 1993 (1991).
[36] L. Kleinman and D. M. Bylander, Phys. Rev. Lett. **48**, 1425 (1982).
[37] P. Hohenberg and W. Kohn, Phys. Rev. **136**, B864 (1965).
[38] R. M. Martin, *Electronic Structure, Basic Theory and Practical Methods* (Cambridge University Press, Cambridge, UK, 2004), p. 145.
[39] L. Hedin, Phys. Rev. **139**, A796 (1965).
[40] M. S. Hybertsen and S. G. Louie, Phys. Rev. B **34**, 5390 (1986).
[41] D. A. Drabold, P. A. Fedders, S. Klemm, and O. F. Sankey, Phys. Rev. Lett. **67**, 2179 (1991).
[42] F. Mauri and R. Car, Phys. Rev. Lett. **75**, 3166 (1995).
[43] G. T. Barkema and N. Mousseau, Phys. Rev. B **62**, 4985 (2000). These authors published only larger models; we use models in this paper that they kindly provided [N. Mousseau (private communication)].
[44] F. Wooten, K. Winer, and D. Weaire, Phys. Rev. Lett. **54**, 1392 (1985).
[45] P. A. Fedders and D. A. Drabold, Phys. Rev. B **47**, 13277 (1993).
[46] R. P. Feynman, Phys. Rev. **56**, 340 (1939).
[47] D. A. Drabold, S. Nakhmanson, and X. Zhang, in *Proceedings of NATO Advanced Study Institute on Properties and Applications of Amorphous Materials, Czech, 2001*, edited by M. F. Thorpe and L. Tichy (Kluwer, London, 2001), p. 221.
[48] X. Zhang and D. A. Drabold, Phys. Rev. Lett. **83**, 5042 (1999).
[49] X. Zhang and D. A. Drabold, Int. J. Mod. Phys. B **15**, 3190 (2001).
[50] J. Li and D. A. Drabold, Phys. Rev. Lett. **85**, 2785 (2000).
[51] P. V. Santos and W. B. Jackson, Phys. Rev. B **46**, 4595 (1992).
[52] R. Atta-Fynn, P. Biswas, and D. A. Drabold, Phys. Rev. B **69**, 245204 (2004).
[53] M. H. Brodsky, M. Cardona, and J. J. Cuomo, Phys. Rev. B **16**, 3556 (1977).
[54] G. Lucovsky, R. J. Nemanich, and J. C. Knights, Phys. Rev. B **19**, 2064 (1979).
[55] W. B. Pollard and G. Lucovsky, Phys. Rev. B **26**, 3172 (1982).
[56] D. A. Drabold, P. A. Fedders, O. F. Sankey, and J. D. Dow, Phys. Rev. B **42**, 5135 (1990).